Telomerase-mediated immortalization of human vaginal wall fibroblasts derived from patients with pelvic organ prolapse

Tao Guo[1], Ting Xie[2], Jinghe Lang[1], Zhijing Sun[1]

[1]Department of Obstetrics and Gynecology, Peking Union Medical College Hospital, Peking Union Medical College, Chinese Academy of Medical Sciences, National Clinical Research Center for Obstetric & Gynecologic Diseases, Beijing 100730, China;
[2]Department of Medical Research Center, Peking Union Medical College Hospital, Chinese Academy of Medical Sciences & Peking Union Medical College, Beijing 100730, China.

Abstract

Background: Extracellular matrix (ECM) remodeling is the most important pathomechanism of pelvic organ prolapse (POP). Fibroblasts are the key to ECM regulation. The passaging capacity of human vaginal wall fibroblasts (hVWFs) is limited *in vitro*. Here, we aimed to immortalize hVWFs through the introduction of human telomerase reverse transcriptase (hTERT).

Methods: Primary cells were derived from the vaginal wall tissue of patients with POP. Cellular senescence was detected via senescence-associated β-galactosidase staining. We employed a lentiviral transfection vector to stably express hTERT in hVWFs at passage 3, generating immortalized hVWFs (i-hVWFs). We then assessed cellular proliferation via the CCK-8 and EdU assays as well as cellular migration via wound healing assays. G-banded chromosome karyotypic analysis was performed to evaluate chromosomal karyotype stability. Finally, cellular tumorigenesis capacity was assessed in nude mice. A two-tailed Student's *t* test was used to compare differences between the two groups.

Results: Our results showed that senescence of primary hVWFs significantly increased from passage seven. From passage 11, hVWFs showed a significantly higher senescence percentage than i-hVWFs. During the continuous passage, i-hVWFs presented stability in proliferation, migration capacity, expression of ECM regulation-related genes, and chromosome karyotype. *In vivo* tumorigenesis was absent in i-hVWFs.

Conclusions: The senescence of hVWFs significantly increased from the seventh passage, and we successfully used hTERT to immortalize hVWFs derived from patients with POP. Studies on POP that require a long-lived hVWF line will benefit from our technique.

Keywords: Pelvic organ prolapse; Fibroblasts; Telomere shortening; Cellular senescence

Introduction

Pelvic organ prolapse (POP) is caused by dysfunction in the supporting tissue of the pelvic floor. The incidence of POP is as high as 3.40% to 10.76% in women.[1] Currently, surgeries are the main effective treatments for POP, and the lifetime risk of undergoing POP surgery is 11.8% to 12.6%.[2,3] Typically, surgeries involve inserting a transvaginal mesh (TVM) to support the sagging organs, but complications associated with TVM (eg, mesh exposure, erosion, and infections) are major obstacles to its application. In 2019, the FDA banned the clinical use of TVM.[4] Thus, researchers are now turning to tissue engineering for the development of effective POP surgery materials.[5-7] Previous studies have seeded fibroblasts on the surface of implanted meshes to improve biocompatibility.[8] However, primary fibroblasts undergo a finite number of cell divisions after *in vitro* culture, and their senescence significantly limits their use in tissue engineering.

Access this article online

Quick Response Code:

Website: www.cmj.org

DOI: 10.1097/CM9.0000000000002278

However, extracellular matrix (ECM) remodeling is the most important pathomechanism of POP. Fibroblasts are critical for regulating the ECM. Thus, researchers have long been concerned with the *in vitro* cellular function of fibroblasts derived from patients with POP.[9-11] However, because of the existing cellular senescence, only primary human vaginal wall fibroblasts (hVWFs) at passages 3 to 6 have been used in most published studies,[12,13] leading to an insufficient number of cells from the same patient to complete a full experiment. Furthermore, cells from different patients are highly heterogeneous, and hence study reproducibility is poor. The availability of hVWFs is also limited because of the scarcity of surgical specimens of vaginal wall tissue and the presence of bacteria in the vaginal environment. The immortalization of hVWFs can help overcome these problems, providing new insights into POP treatment and the associated mechanisms.

Correspondence to: Prof. Jinghe Lang, Department of Obstetrics and Gynecology, Peking Union Medical College Hospital, Shuaifuyuan No. 1, Dong-Cheng District, Beijing 100730, China
E-Mail: langjh@hotmail.com;
Prof. Zhijing Sun, Department of Obstetrics and Gynecology, Peking Union Medical College Hospital, Shuaifuyuan No. 1, Dong-Cheng District, Beijing 100730, China
E-Mail: sunzhj2001@sina.com

Chinese Medical Journal 2023;136(5)
Received: 18-05-2022; **Online:** 13-03-2023 **Edited by:** Yanjie Yin

An important mechanism of immortalization is overcoming telomere shortening, which is the main cause of cell senescence. The telomere length is maintained through the activity of telomerase, which comprises human telomerase reverse transcriptase (hTERT) and an ribonucleic acid (RNA) template. Although this RNA template is highly conserved, the hTERT level is negative or below the threshold level of enzyme activity in most human somatic cells.[14] Thus, several studies have attempted immortalization by introducing hTERT into normal somatic cells, including epithelial cells of renal proximal tubules, bone mesenchymal stromal cells, and hepatocytes.[15-17] However, no similar attempt has been made with hVWFs. This study aimed to validate the hTERT method with hVWFs derived from patients with POP. We then examined cellular proliferation, migration, key protein expression, chromosome karyotypic stability, and the *in vivo* tumorigenesis capacity of hTERT-treated hVWFs.

Methods

Ethical approval

The study was conducted according to the guidelines of the *Declaration of Helsinki*, and approved by the Ethics Committee of our institution (No. JS-2240, 25/02/2020). Explicit written informed consents were signed by participants.

Isolation and culture of primary hVWF

Vaginal wall tissues were collected from patients who underwent surgery for anterior vaginal wall prolapses at our institution. Patients with stage III or IV anterior vaginal wall prolapses according to the Pelvic Organ Prolapse Quantification were included.

A piece of about 1 cm^2 tissue from the prolapse site of the anterior vaginal wall was collected during surgery. The tissue was placed in 4°C Dulbecco's modified Eagle's medium (DMEM; Gibco, Carlsbad, CA, USA) and immediately transported to the laboratory. Tissues were washed with phosphate-buffered saline (PBS, ServiceBio, Wuhan, China), cut into pieces smaller than 2 mm, and then incubated with 10 mg/mL collagenase I (Sigma, St. Louis, MO, USA) at 37°C for 2 h. The DMEM with 10% fetal bovine serum (FBS; Gibco) was added to terminate the digestion. The digestion liquid was filtered using a filter screen with a 75 μm pore size. The liquid was then centrifuged at 1000 × *g* for 5 min. Cells at the bottom of the centrifuge tube were then suspended in DMEM with 10% FBS and cultured at 37°C with 5% CO_2. In the subsequent culture process, cells were passed in a ratio of 1:3.

Immunofluorescent staining

Cells were cultured in a dish (Beyotime; Shanghai, China) that had a glass bottom designed for confocal laser photography. Cells were fixed in 4% paraformaldehyde (Beyotime) for 20 min and washed three times with PBS. Immunostaining permeabilization buffer (Beyotime) was added for cell permeabilization and the antigen was blocked by immunostaining blocking buffer (Beyotime) according to the manufacturer's instructions. The primary antibodies of FSP-1 (1:200, ZSGB-Bio, Beijing, China), Vimentin (1:200, ZSGB-Bio), ACTA2 (1:200, ZSGB-Bio), CK5/6 (1:200, ZSGB-Bio), and hTERT (1:200, Solarbio; Beijing, China) were added and incubated at 4°C overnight (>12 h) and washed three times with PBS. Secondary antibodies (1:500, Beyotime) were incubated for 2 h at room temperature and washed three times with PBS. Then, 5 μg/mL 4,6-Diamidino-2-phenylindole (DAPI) was incubated for 5 min and washed three times with PBS. Fluorescence observing and imaging were performed using a confocal laser scanning microscope (Ti2-E/A1R+; Nikon, Tokyo, Japan).

Senescence-associated β-galactosidase (SA-β-gal) staining

Cell senescence was detected with SA-β-gal staining. Cells were seeded into six-well plates and cultured until they reached 50% confluence. We used an SA-β-gal staining kit supplied by Beyotime. SA-β-gal staining was performed according to the manufacturer's instructions. Briefly, cells were fixed with the fixative in the kit at room temperature and incubated with the staining solution at 37°C overnight (>12 h). Cells were observed and photographed using an optical microscope (Ti2-U; Nikon, Tokyo, Japan).

Lentivirus construction and transfection

We overexpressed the hTERT gene in hVWF using lentiviral vectors. The lentiviral vectors carrying green fluorescent protein, puromycin resistance, and target gene were purchased from GENECHEM (Shanghai, China). Empty lentiviruses without target genes served as the negative control. Before transfection, cells were seeded into six-well plates and cultured until 30% confluence. Then, cells were cultured in the DMEM with lentiviral vectors for 12 h and the culture medium was then changed to normal DMEM with 10% FBS. When cells reached 90% confluence, puromycin (GENECHEM) was added with a 2 μg/mL concentration to screen cell lines with stable overexpression of hTERT.

Western blotting (WB)

Cells were washed with 4°C PBS and lysed in lysis buffer (Beyotime) with protease and phosphatase inhibitors (Beyotime). Lysates were centrifuged at 12,500 × *g* and 4°C for 15 min. Supernatants were collected and proteins were denatured with the NuPAGE® LDS Sample Buffer (4×) (Invitrogen; Carlsbad, CA, USA). Proteins were separated on 10% sodium dodecyl sulfate (SDS)-polyacrylamide gels and transferred onto polyvinylidene difluoride (PVDF, Invitrogen) membranes using an iBlot® Gel Transfer Device (Invitrogen). Membranes were blocked in 5% skimmed milk and then incubated with specific antibodies including hTERT (1:1000; Solarbio), COL1A1 (1:1000; ABclonal; Wuhan China), COL3A1 (1:1000; ABclonal), ELN (1:1000; ABclonal), MMP2 (1:1000; Abcam; Cambridge, UK), MMP3 (1:1000; Abcam), MMP9 (1:1000; Abcam), TIMP1 (1:1000; ABclonal), TIMP2 (1:1000; ABclonal), and GAPDH (1:1000; Abcam). Then, membranes were incubated with horseradish peroxidase (HRP)-conjugated secondary anti-

bodies (Solarbio) at room temperature for 2 h. Rapid Step ECL Reagent (Millipore, Schwalbach, Germany) was used to visualize the immunoblot.

Real-time quantitative PCR (RT-qPCR)

The culture medium was removed and cells were washed using 4°C PBS. Total RNA was isolated using FastPure Cell/Tissue Total RNA Isolation Kit V2 (Vazyme Biotech, Nanjing, China) according to the manufacturer's instructions, and cDNA was synthesized using HiScript III RT SuperMix for quantitative polymerase chain reaction (qPCR) (Vazyme). A Taq Pro Universal SYBR qPCR Master Mix (Vazyme) was used to perform RT-qPCRs in the CFX Connect (Bio-Rad; Hercules, CA, USA). GAPDH was used as the internal control and the relative gene expression was calculated using the 2-ΔΔCT method. The PCR primers were purchased for the Tsingke Biotechnology (Beijing, China) and listed in Supplementary Table 1, http://links.lww.com/CM9/B264.

Cell counting kit 8 (CCK-8) assays

Cells were seeded into 96-well plates at a density of 4×10^3 per well. CCK-8 solution (Dojindo, Kumamoto, Japan) was added and incubated for 45 min. Absorbance at 450 nm was measured using the Thermo Fisher Varioskan Flash (Thermo Fisher, CA, USA) microplate reader.

EdU assays

Cells were seeded into 6-well plates at a density of 6×10^5 per well and cultured to 50% confluence. An EdU Cell Proliferation Kit (Beyotime) was used. Cells were incubated with 10 mmol/L EdU at 37°C for 2 h and the positive cells were detected according to the manufacturer's instructions.

Wound healing assays

A device Culture-Inserts (Ibidi GmbH, Munich, Germany) was used to perform wound healing assays according to the manufacturer's instructions. Briefly, the Culture-Inserts were placed in the 6-well plates, and 70 μL cell suspension containing 3×10^4 cells was added to each well of the Culture-Inserts. After cell attachment, the Culture-Inserts were removed and approximately 500 μm cell-free gap was formed. Then, cells were cultured with the serum-free medium for 36 h. Cells were observed and photographed using an optical microscope (Nikon).

G-banded chromosome karyotypic analysis

We adopted a classical method for chromosome karyotype analysis. Briefly, cultured cells were treated with colchicine (Beyotime) for 2 h before harvesting. Next, cells were incubated with a hypotonic potassium chloride solution (Beyotime) at 37°C for 15 min. A fixative mixture of methanol and glacial acetic acid (Beijing Chemical Works, Beijing, China) was then used to fix the cells. The cell suspension was then dripped onto slides and baked at 80°C for 2 h. Finally, cells were digested with trypsin (Gibco), and Giemsa (Beyotime) staining was performed. Image acquisition and data analysis were performed by KaYouTaiPu (Hang Zhou, China).

In vivo tumorigenesis assays

All animal research procedures were approved by the Institution of Animal Care and Committee at our institution. Six-week-old female BALB/c nude mice were purchased from the Vital River (Beijing, China). For subcutaneous tumor transplantation, 1×10^6 cells in 100 μL were injected subcutaneously into the armpit of nude mice ($n = 5$ per group). Immortalized hVWF (I-hVWF) was injected to evaluate the tumorigenesis and HeLa cells were injected as a control group to ensure technical correctness. Six weeks after injection, mice were killed and tumors were measured and photographed.

Statistical analysis

Statistical analyses were performed using GraphPad Prism 8 (GraphPad Software, Inc., CA, USA). Data were presented as the mean with the standard deviation (SD). A two-tailed Student's t test was used to compare differences between the two groups. Statistical significance was defined as $P < 0.05$.

Results

Isolation and senescence evaluation of primary fibroblasts

We isolated primary fibroblasts from vaginal wall tissues of women with POP and cultured them for three passages. Subsequently, fibroblasts were identified through immunofluorescent staining. Isolated cells were positive for FSP-1 and vimentin but negative for CK5/6 and ATCA2, indicating that they were neither epithelial nor muscle cells [Figure 1]. Therefore, we concluded that our cultured cells were hVWFs.

We found that hVWFs could be serially cultured *in vitro* for 16–18 passages. However, as the passage count increased, more cells grew in volume and exhibited proliferation arrest. Therefore, we performed SA-β-gal staining to evaluate the hVWFs senescence percentage at different passages. Overall, the percentage of SA-β-gal-positive cells gradually increased with an increase in the number of passages [Figure 2A]. We observed no difference in the percentage of positive cells ($P = 0.261$) between passages 3 and 5, but starting from passage 7, the percentage of positive cells significantly increased compared to the passage 3 levels ($P = 0.011$). At passage 18, nearly 100% hVWFs were SA-β-gal-positive [Figure 2B] and cell growth stopped.

Overexpressing hTERT protein in hVWFs

We used a lentiviral transfection vector to stably overexpress hTERT protein in hVWFs. Transfection was performed at passage three. According to RT-qPCR, hTERT mRNA expression was negative in hVWFs but positive in i-hVWFs, being 0.012 compared with GAPDH [Figure 3A]. WB then showed that the expression of hTERT protein in i-hVWFs was 18.36-fold than in

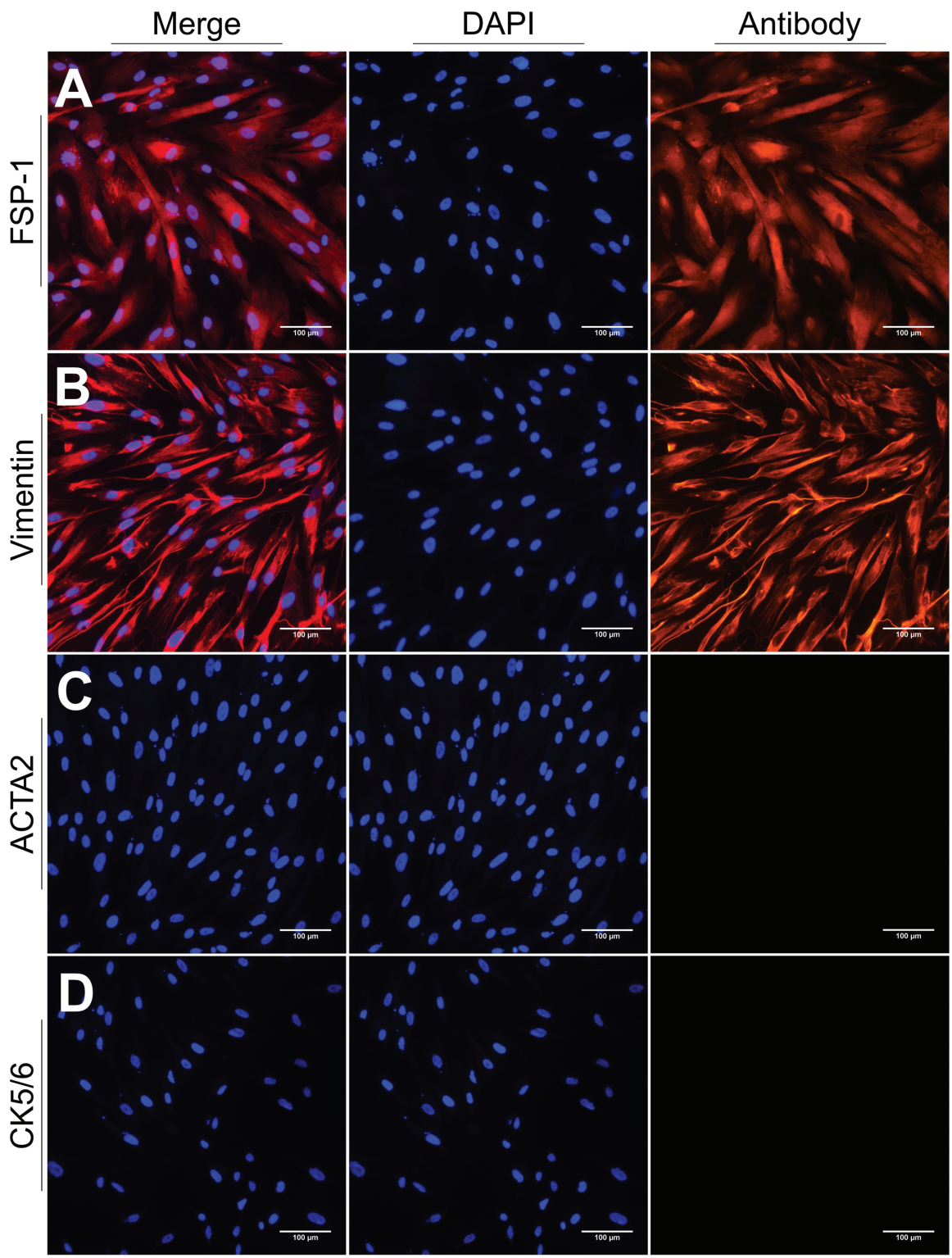

Figure 1: Identification of hVWFs by immunofluorescent staining. (A) FSP-1; (B) Vimentin; (C) Smooth Muscle alpha-actin (ACTA2); (D) Keratin 5/6 (CK5/6). Scale bar = 100 μm. FSP-1: Fibroblast-specific protein-1; hVWFs: Human vaginal wall fibroblasts.

hVWFs [Figure 3B]. Immunofluorescence staining confirmed that the hTERT protein was localized in the cell nucleus [Figure 3C], as expected. The control group without hTERT antibodies showed negative results, indicating a lack of non-specific binding with secondary antibodies.

Cell senescence evaluation of i-hVWFs

After culturing i-hVWFs *in vitro*, we compared their senescence with hVWF senescence at different passages. The percentage of SA-β-gal-positive i-hVWFs gradually increased, but pairwise comparisons between two contiguous passages did not differ. After passage 11, the

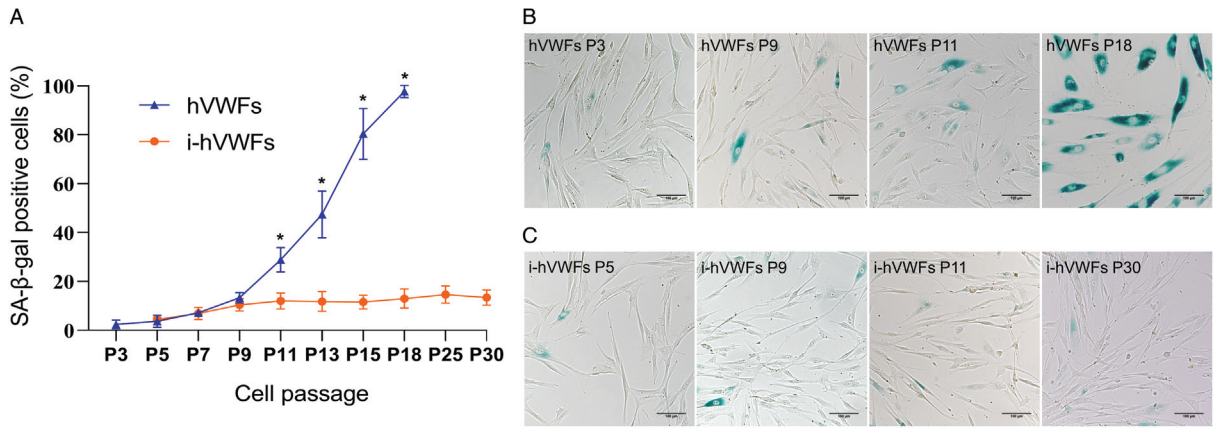

Figure 2: SA-β-gal staining of hVWFs and i-hVWFs at different passages. (A) Statistical analysis of SA-β-gal staining positive percentage of hVWFs and i-hVWFs in different passages; (B) Representative pictures for SA-β-gal staining of hVWFs at P3, P9, P11, and P18; (C) Representative pictures for SA-β-gal staining of i-hVWFs at P5, P9, P11, and P30. *Indicates $P < 0.05$. Scale bar = 100 μm. hVWFs: Human vaginal wall fibroblasts; i-hVWFs: Immortalized hVWFs; SA-β-gal: Senescence-associated β-galactosidase.

percentage of positive i-hVWFs eventually stabilized between 12.8% and 15.4% [Figure 2A,C].

At passages 5, 7, and 9, i-hVWFs and hVWFs did not differ in the percentage of SA-β-gal-positive cells ($P = 0.488$, 0.816, and 0.262, respectively). However, at passage 11, significantly more hVWFs than i-hVWFs were found to be SA-β-gal-positive ($P = 0.014$). In all subsequent passages, the percentage of senescence was significantly higher in hVWFs than in i-hVWFs. In addition, the control group transfected with a negative control lentiviral transfection vector exhibited senescence curves similar to those of hVWFs [Supplementary Figure 1, http://links.lww.com/CM9/B264].

Proliferation and migration of hVWFs and i-hVWFs

At passage 5, CCK-8 assays showed that hVWF and i-hVWF proliferation did not significantly differ (Figure 4A; $P = 0.146$). EdU assays confirmed the lack of any significant changes (Figure 4D; $P = 0.805$). Wound healing assays (Figure 4G; $P = 0.418$) also did not reveal differences between i-hVWFs and hVWFs at passage 5. Therefore, hTERT overexpression in hVWFs did not affect cellular proliferation or migration.

Because the percentage of i-hVWF senescence significantly decreased from the eleventh passage on, we compared the proliferation and migration of i-hVWFs and hVWFs at passage 11. In CCK-8 assays [Figure 4B], hVWFs had a significantly lower proliferation rate than i-hVWFs ($P = 0.013$). These changes were confirmed via EdU assays (Figure 4E; $P < 0.001$). Moreover, hVWFs migrated less than i-hVWFs at passage 11 (Figure 4H; $P < 0.001$).

We then compared i-hVWF proliferation and migration across different passages. Neither CCK-8 (Figure 4A–C, $P = 0.923$) nor EdU assays (Figure 4D–F, $P = 0.791$) revealed a significant difference in i-hVWF proliferation between passages 5, 11, 20, and 30. Wound healing assays also indicated that the i-hVWF migration ability was stable in these four passages (Figure 4G–I, $P = 0.195$).

Expression of representative proteins in i-hVWFs

Human VWFs play an important role in regulating ECM components. Thus, we performed RT-qPCR and WB assays to evaluate the relative expression of ECM components, including collagen type I alpha 1 chain (*COL1A1*), collagen type 3 alpha 1 chain (*COL3A1*), elastin (*ELN*), matrix metalloproteinase 2 (*MMP2*), *MMP3*, *MMP9*, tissue inhibitors of metalloproteinase 1 (*TIMP1*), and *TIMP2*. Their expression in i-hVWFs was compared between passages 5, 10, 20, and 30. *COL1A1*, *COL3A1*, *ELN*, *MMP2*, *MMP3*, *MMP9*, *TIMP1*, and *TIMP2* were stably expressed and showed no significant differences at mRNA ($P = 0.673$, 0.288, 0.745, 0.250, 0.389, 0.688, 0.127, and 0.274, respectively) or protein ($P = 0.628$, 0.063, 0.146, 0.298, 0.230, 0.668, 0.093, and 0.169, respectively) levels [Figure 5].

Karyotype stability in i-hVWFs

Karyotype stability was analyzed using G-band chromosome karyotypic analysis. Both results of hVWFs [Figure 6A] and i-hVWFs [Figure 6B] revealed a normal female karyotype.

In vivo tumorigenesis of i-hVWFs

The results of tumorigenesis assays using nude mice showed that i-hVWFs could not form tumors [Figure 6C]. In the HeLa-injected control group, all five mice developed tumors (mean diameter = 0.83 cm, range = 0.71–0.98 cm) at the injection site [Figure 6D].

Discussion

In this study, we described hVWF senescence *in vitro* and validated the hTERT immortalization method for hVWFs.

In vitro cellular senescence includes replicative senescence (RS) and stress-induced premature senescence (SIPS). Whereas the former is caused by telomere shortening, multiple factors influence SIPS, such as abnormal concentrations of nutrients or growth factors in the

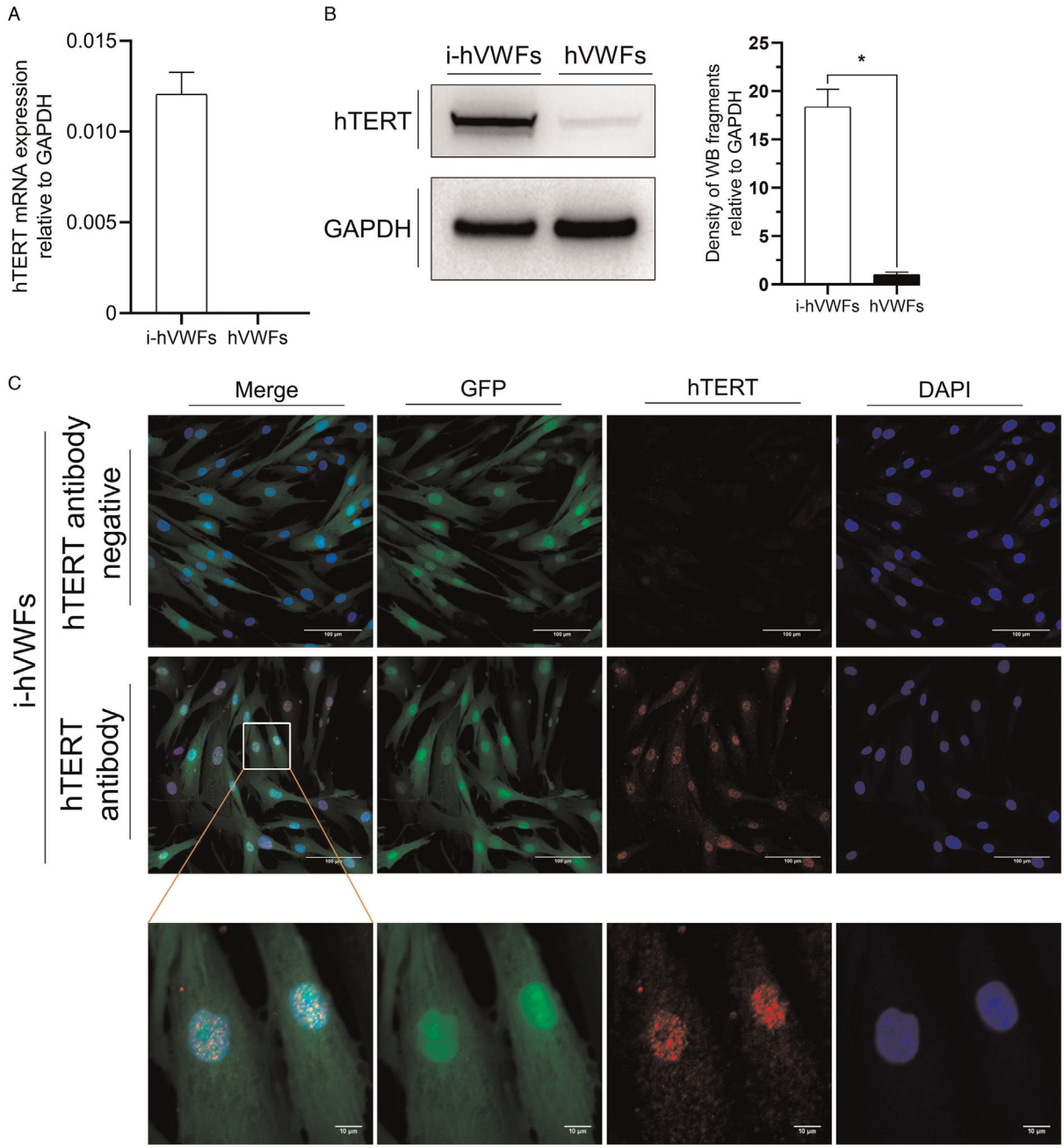

Figure 3: Overexpression and location of hTERT protein in hVWFs. (A) Evaluation of relative hTERT mRNA expression relative to GAPDH in i-hVWFs and hVWFs by RT-qPCR analysis; (B) Evaluation of hTERT protein expression in i-hVWFs and hVWFs by WB analysis; (C) Evaluation of hTERT protein expression and location of hTERT protein by immunofluorescent staining. *Indicates $P < 0.05$. Scale bar = 100 μm and scale bar = 10 μm in the enlarged image. GFP: Green fluorescent protein; hTERT: Human telomerase reverse transcriptase; hVWFs: Human vaginal wall fibroblasts; i-hVWFs: Immortalized hVWFs; RT-qPCR: Real-time quantitative polymerase chain reaction; WB: Western blotting.

culture medium, differences in O_2 levels, and the absence of ECM components.[18] Here, we found that the *in vitro* senescence ratio of hVWFs increased with the increase in cell passage. Cells at passage five did not differ from cells at passage three, with both exhibiting a mean senescence percentage as low as 3.7%. However, starting at passage seven, cellular senescence significantly increased. Therefore, we conclude that if senescence is expected to be a factor in research using primary hVWFs derived from POP patients, the cells should not go beyond the seventh passage. In addition, after hTERT overexpression, i-hVWFs showed a significantly lower percentage of cellular senescence starting from passage 11, coinciding with the beginning of RS in hVWFs. Eventually, i-hVWFs achieved a stable cellular senescence percentage between 12.0% and 14.6%, representing SIPS.

Prior to hTERT, oncogenes were frequent candidates to induce immortalization in normal cells. Commonly used oncogenes include human papillomavirus (HPV) 16 E6/E7 and simian virus 40 large T antigens (SV40 Tag), but both can induce malignant transformation and cause

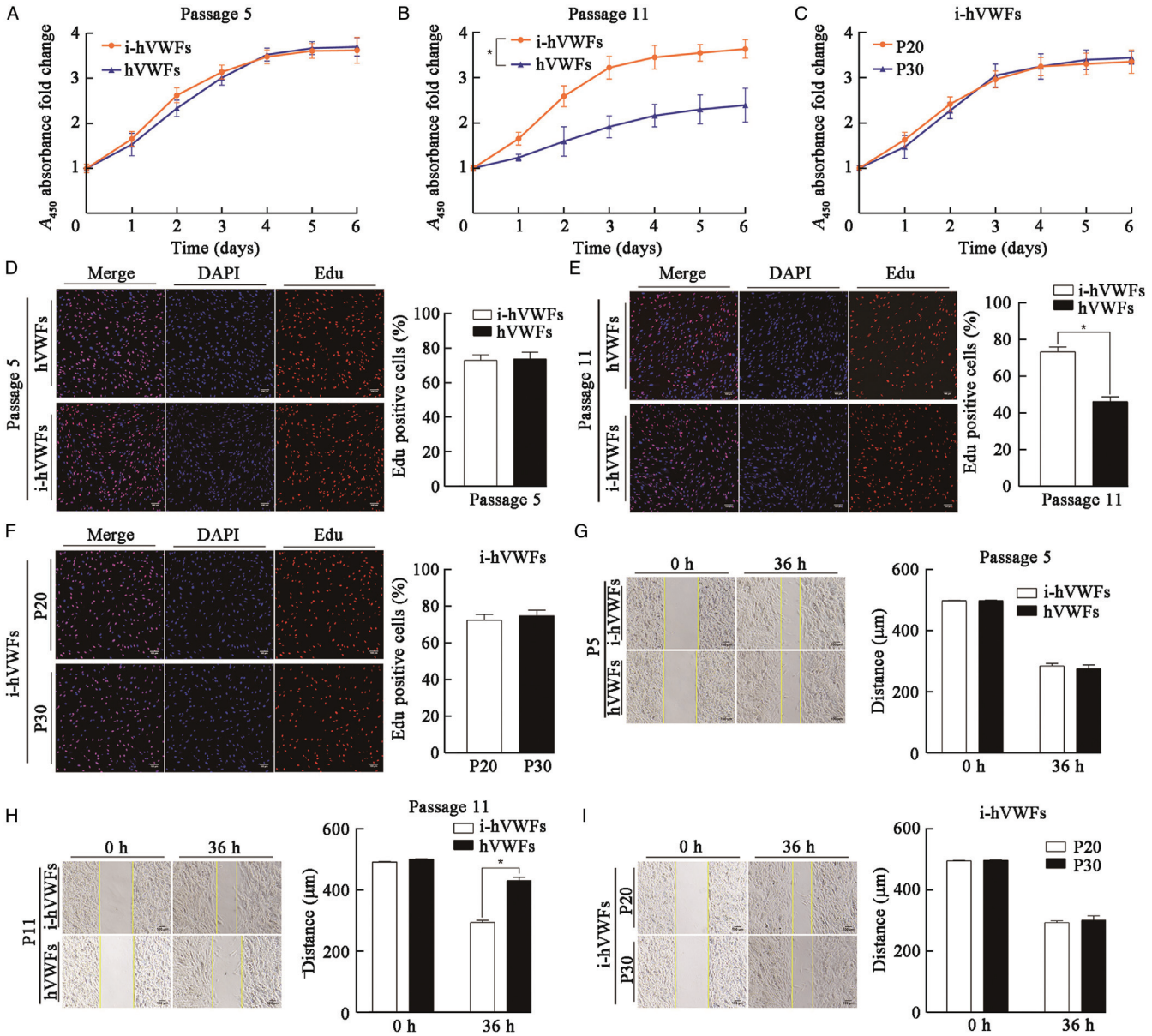

Figure 4: Cell proliferation and migration of i-hVWFs and hVWFs at different passages. CCK-8 assays for cell proliferation of i-hVWFs and hVWFs at passage 5 (A) and 11 (B). CCK-8 assays for cell proliferation of i-hVWFs at passages 20 and 30 (C). EdU assays for cell proliferation comparison between hVWFs and i-hVWFs at passage 5 (D) and passage 11 (E). (F) EdU assays for cell proliferation comparison between passages 20 and 30 of i-hVWFs; Wound healing assays for cell migratory abilities of i-hVWFs and hVWFs at passages 5 (G) and 11 (H). Wound healing assays for cell migratory abilities of i-hVWFs at passages 20 and 30 (I). *Indicates $P < 0.05$. Scale bar = 100 μm. CCK-8: Cell counting kit 8; hVWFs: Human vaginal wall fibroblasts; i-hVWFs: Immortalized hVWFs.

tumorigenesis *in vivo*.[19] In the 1990s, Bodnar *et al*[20] introduced immortalization through the expression of hTERT protein in hTERT-negative somatic human cells. Compared with oncogenes, hTERT-immortalized cells usually present with better karyotypic and phenotypic stability, along with weaker tumorigenesis capacity.[15,16,19,21] Given these advantages, we adopted the hTERT immortalization method in this study. The i-hVWF line has been cultured for over 50 passages in our laboratory. We also used a short tandem repeat (STR) analysis to rule out the possibility of contamination by other cells [Supplementary Table 2, http://links.lww.com/CM9/B264]. Radiation is another method for immortalizing cells. However, as with oncogenes, it can cause significant changes in genetic material, malignant transformation, and tumorigenesis *in vivo*.[22]

The most important pathomechanism of POP is ECM remodeling. The vaginal wall tissues or uterine ligaments of patients with POP patients express *MMP2* and *MMP9* at high levels, whereas *COL1*, *COL3*, *TIMP1*, and *TIMP2* are present at low levels.[9,10,23-25] Previously, our group profiled the single-cell transcriptome of vaginal wall cells to reveal that POP-derived hVWFs mainly differed in the expression of ECM regulation-related mRNA.[26] Other researchers have also found that the expression levels of ECM components and ECM

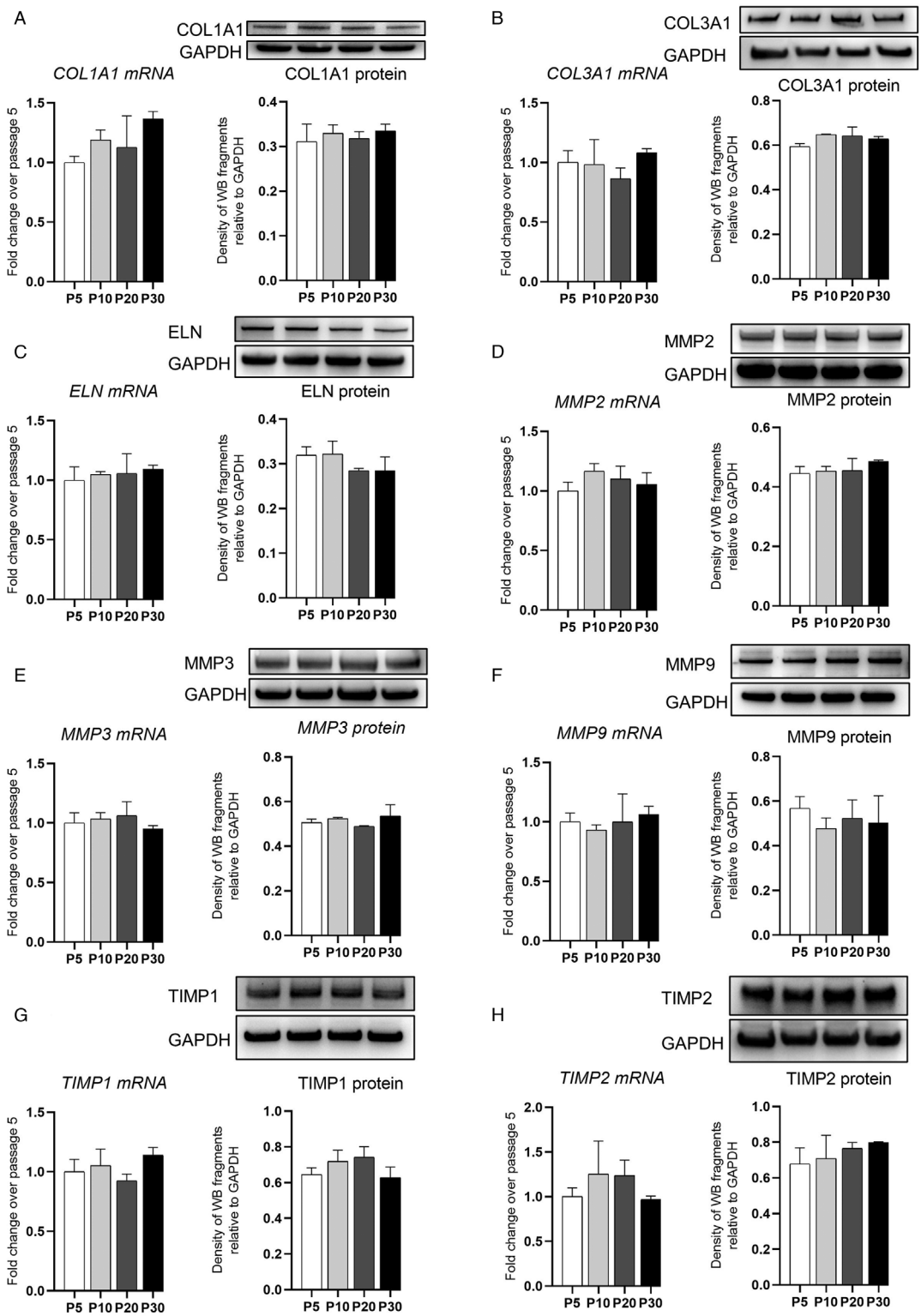

Figure 5: Representative gene expression of i-hVWFs at different passages. RT-qPCR for mRNA expression and western blotting for protein expression of COL1A1 (A), COL3A1 (B), ELN (C), MMP2 (D), MMP3 (E), MMP9 (F), TIMP1 (G), and TIMP2 (H) at passage 5, 10, 20, and 30, respectively. Scale bar = 100 μm. COL1A1: Collagen type I alpha 1 chain; GAPDH: Glyceraldehyde 3-phosphate dehydrogenase; i-hVWFs: Immortalized hVWFs; MMP2: Matrix metalloproteinase 2; RT-qPCR: Real-time quantitative PCR; TIMP1: Tissue inhibitors of metalloproteinase 1.

regulatory enzymes are significantly altered with cellular senescence.[27,28] Thus, when hVWFs are immortalized, a key phenotype to be assessed is the stable expression of genes involved in ECM regulation. Here, both RT-qPCR and Western blots confirmed that hTERT overexpression in hVWFs did not affect ECM-related gene expression during the continuous passage.

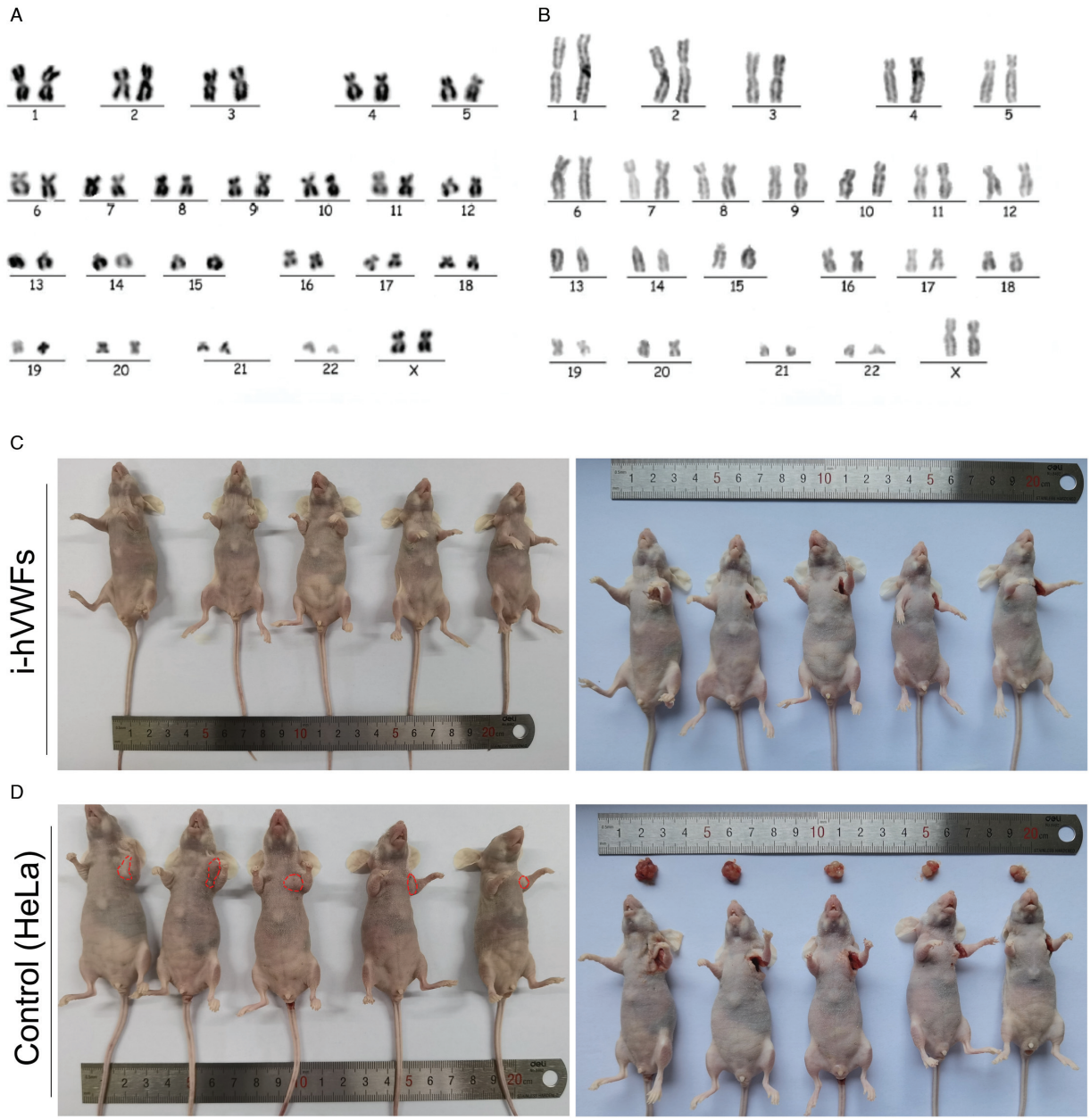

Figure 6: Representative pictures for G-band chromosome karyotypic analysis of hVWFs at passage 3 (A) and i-hVWFs (B) at passage 30. *In vivo* tumorigenesis assays for i-hVWFs (C) and HeLa cells as the control group (D). hVWFs: Human vaginal wall fibroblasts; i-hVWFs: Immortalized hVWFs.

Tumor-like activities are a common concern with immortalized somatic cells. The loss of contact inhibition is an important feature of many cancer cells,[29] and this characteristic has been reported in some hTERT-immortalized cells.[30,31] In this study, i-hVWFs exhibited normal monolayer proliferation. Furthermore, CCK-8 assays indicated obvious contact inhibition from the fourth day for both primary hVWFs and i-hVWFs. We did not observe any malignant transformation or tumorigenesis with i-hVWFs.

In conclusion, we successfully used the hTERT introduction to immortalize hVWFs derived from patients with POP. We revealed that the percentage of primary hVWF senescence significantly increased from passage seven. We also demonstrated that i-hVWFs were similar to primary cells in terms of proliferation, migration, and the expression of key genes. I-hVWFs also had a stable chromosome karyotype and low capacity for *vivo* tumorigenesis. We suggest that our i-hVWF line could serve as an *in vitro* POP model for future studies that require long-lived cells.

Funding

This study was supported by the grants from the National Natural Science Foundation of China (No.81971366), the Beijing Natural Science Foundation (No.Z190021), and CAMS Innovation Fund for Medical Sciences (No. CIFMS 2020-I2M-C&T-B-043).

Conflicts of interest

None.

References

1. Mou T, Warner K, Brown O, Yeh C, Beestrum M, Kenton K, *et al*. Prevalence of pelvic organ prolapse among US racial populations: a systematic review and meta-analysis of population-based screening studies. Neurourol Urodyn 2021;40:1098–1106. doi: 10.1002/nau.24672.
2. Wu JM, Matthews CA, Conover MM, Pate V, Funk MJ. Lifetime risk of stress urinary incontinence or pelvic organ prolapse surgery. Obstet Gynecol 2014;123:1201–1206. doi: 10.1097/aog.0000000000000286.
3. Fialkow MF, Newton KM, Lentz GM, Weiss NS. Lifetime risk of surgical management for pelvic organ prolapse or urinary incontinence. Int Urogynecol J Pelvic Floor Dysfunct 2008;19:437–440. doi: 10.1007/s00192-007-0459-9.
4. Holt Ed. US FDA rules manufacturers to stop selling mesh devices. Lancet 2019;393:1686. doi: 10.1016/s0140-6736(19)30938-9.
5. Cazorla-Luna R, Ruiz-Caro R, Veiga MD, Malcolm RK, Lamprou DA. Recent advances in electrospun nanofiber vaginal formulations for women's sexual and reproductive health. Int J Pharm 2021;607:121040. doi: 10.1016/j.ijpharm.2021.121040.
6. Paul K, Darzi S, Werkmeister JA, Gargett CE, Mukherjee S. Emerging nano/micro-structured degradable polymeric meshes for pelvic floor reconstruction. Nanomaterials 2020;10:1120. doi: 10.3390/nano10061120.
7. Mangir N, Aldemir Dikici B, Chapple CR, MacNeil S. Landmarks in vaginal mesh development: polypropylene mesh for treatment of SUI and POP. Nat Rev Urol 2019;16:675–689. doi: 10.1038/s41585-019-0230-2.
8. Boennelycke M, Gras S, Lose G. Tissue engineering as a potential alternative or adjunct to surgical reconstruction in treating pelvic organ prolapse. Int Urogynecol J 2013;24:741–747. doi: 10.1007/s00192-012-1927-4.
9. Chen YS, Wang XJ, Feng W, Hua KQ. Advanced glycation end products decrease collagen I levels in fibroblasts from the vaginal wall of patients with POP via the RAGE, MAPK and NF-(B pathways. Int J Mol Med 2017;40:987–998. doi: 10.3892/ijmm.2017.3097.
10. Zhang Q, Liu C, Hong S, Min J, Yang Q, Hu M, *et al*. Excess mechanical stress and hydrogen peroxide remodel extracellular matrix of cultured human uterosacral ligament fibroblasts by disturbing the balance of MMPs/TIMPs via the regulation of TGF-(1 signaling pathway. Mol Med Rep 2017;15:423–430. doi: 10.3892/mmr.2016.5994.
11. Yin Y, Han Y, Shi C, Xia Z. IGF-1 regulates the growth of fibroblasts and extracellular matrix deposition in pelvic organ prolapse. Open Med 2020;15:833–840. doi: 10.1515/med-2020-0216.
12. Vashaghian M, Ruiz-Zapata AM, Kerkhof MH, Zandieh-Doulabi B, Werner A, Roovers JP, *et al*. Toward a new generation of pelvic floor implants with electrospun nanofibrous matrices: A feasibility study. Neurourol Urodyn 2017;36:565–573. doi: 10.1002/nau.22969.
13. Zhu Y, Li L, Xie T, Guo T, Zhu L, Sun Z. Mechanical stress influences the morphology and function of human uterosacral ligament fibroblasts and activates the p38 MAPK pathway. Int Urogynecol J 2022;33:2203–2212. doi: 10.1007/s00192-021-04850-7.
14. Shay JW, Bacchetti S. A survey of telomerase activity in human cancer. Eur J Cancer 1997;33:787–791. doi: 10.1016/s0959-8049(97)00062-2.
15. Wieser M, Stadler G, Jennings P, Streubel B, Pfaller W, Ambros P, *et al*. hTERT alone immortalizes epithelial cells of renal proximal tubules without changing their functional characteristics. Am J Physiol Renal Physiol 2008;295:F1365–F1375. doi: 10.1152/ajprenal.90405.2008.
16. An K, Liu HP, Zhong XL, Deng DYB, Zhang JJ. Liu ZH. hTERT-immortalized bone mesenchymal stromal cells expressing rat galanin via a single tetracycline-inducible lentivirus system. Stem Cells Int 2017;2017:6082684. doi: 10.1155/2017/6082684.
17. Ramboer E, De Craene B, De Kock J, Vanhaecke T, Berx G, Rogiers V, *et al*. Strategies for immortalization of primary hepatocytes. J Hepatol 2014;61:925–943. doi: 10.1016/j.jhep.2014.05.046.
18. Mohamad Kamal NS, Safuan S, Shamsuddin S, Foroozandeh P. Aging of the cells: insight into cellular senescence and detection methods. Eur J Cell Biol 2020;99:151108. doi: 10.1016/j.ejcb.2020.151108.
19. Wang Y, Chen S, Yan Z, Pei M. A prospect of cell immortalization combined with matrix microenvironmental optimization strategy for tissue engineering and regeneration. Cell Biosci 2019;9:7. doi: 10.1186/s13578-018-0264-9.
20. Bodnar AG, Ouellette M, Frolkis M, Holt SE, Chiu CP, Morin GB, *et al*. Extension of life-span by introduction of telomerase into normal human cells. Science 1998;279:349–352. doi: 10.1126/science.279.5349.349.
21. Song Y, Joshi NR, Vegter E, Hrbek S, Lessey BA, Fazleabas AT. Establishment of an immortalized endometriotic stromal cell line from human ovarian endometrioma. Reprod Sci 2020;27:2082–2091. doi: 10.1007/s43032-020-00228-0.
22. Gudjonsson T, Villadsen R, Rønnov-Jessen L, Petersen OW. Immortalization protocols used in cell culture models of human breast morphogenesis. Cell Mol Life Sci 2004;61:2523–2534. doi: 10.1007/s00018-004-4167-z.
23. Liu C, Wang Y, Li BS, Yang Q, Tang JM, Min J, *et al*. Role of transforming growth factor (-1 in the pathogenesis of pelvic organ prolapse: a potential therapeutic target. Int J Mol Med 2017;40:347–356. doi: 10.3892/ijmm.2017.3042.
24. Ruiz-Zapata AM, Kerkhof MH, Zandieh-Doulabi B, Brölmann HA, Smit TH, Helder MN. Functional characteristics of vaginal fibroblastic cells from premenopausal women with pelvic organ prolapse. Mol Hum Reprod 2014;20:1135–1143. doi: 10.1093/molehr/gau078.
25. Zhu YP, Xie T, Guo T, Sun ZJ, Zhu L, Lang JH. Evaluation of extracellular matrix protein expression and apoptosis in the uterosacral ligaments of patients with or without pelvic organ prolapse. Int Urogynecol J 2021;32:2273–2281. doi: 10.1007/s00192-020-04446-7.
26. Li Y, Zhang QY, Sun BF, Ma Y, Zhang Y, Wang M, *et al*. Single-cell transcriptome profiling of the vaginal wall in women with severe anterior vaginal prolapse. Nat Commun 2021;12:87. doi: 10.1038/s41467-020-20358-y.
27. Ritschka B, Storer M, Mas A, Heinzmann F, Ortells MC, Morton JP, *et al*. The senescence-associated secretory phenotype induces cellular plasticity and tissue regeneration. Genes Dev 2017;31:172–183. doi: 10.1101/gad.290635.116.
28. Perrott KM, Wiley CD, Desprez PY, Campisi J. Apigenin suppresses the senescence-associated secretory phenotype and paracrine effects on breast cancer cells. Geroscience 2017;39:161–173. doi: 10.1007/s11357-017-9970-1.
29. McClatchey AI, Yap AS. Contact inhibition (of proliferation) redux. Curr Opin Cell Biol 2012;24:685–694. doi: 10.1016/j.ceb.2012.06.009.
30. Burns JS, Abdallah BM, Guldberg P, Rygaard J, Schrøder HD, Kassem M. Tumorigenic heterogeneity in cancer stem cells evolved from long-term cultures of telomerase-immortalized human mesenchymal stem cells. Cancer Res 2005;65:3126–3135. doi: 10.1158/0008-5472.Can-04-2218.
31. Serakinci N, Guldberg P, Burns JS, Abdallah B, Schrødder H, Jensen T, *et al*. Adult human mesenchymal stem cell as a target for neoplastic transformation. Oncogene 2004;23:5095–5098. doi: 10.1038/sj.onc.1207651.

How to cite this article: Guo T, Xie T, Lang J, Sun Z. Telomerase-mediated immortalization of human vaginal wall fibroblasts derived from patients with pelvic organ prolapse. Chin Med J 2023;136:578–587. doi: 10.1097/CM9.0000000000002278